Inorganic Chemistry
Article
Cite This: Inorg. Chem. 2020, 59, 555−562
pubs.acs.org/IC

Theoretical Probe to the Mechanism of Pt-Catalyzed C−H Acylation Reaction: Possible Pathways for the Acylation Reaction of a Platinacycle

Elizabeth Warden, Libero Bartolotti, Shouquan Huo,* and Yumin Li*

Department of Chemistry, East Carolina University, Greenville, North Carolina 27858, United States

Supporting Information

ABSTRACT: Density functional theory (DFT) and nudged elastic band (NEB) theory have been used to study the possible pathways for the acylation of cycloplatinated complex **A** derived from 2-phenoxypyridine, which is conceived as the key step in the platinum-catalyzed acylation of 2-aryloxypyridines. Geometry optimization indicates that the previously proposed intermediate, an arenium ion species as a result of analogous aromatic substitution, is not an energy minimum, but rather cationic Pt-arene η^2-complex **E** is obtained as a stable intermediate. NEB simulations suggest that the minimum energy pathway for the acylation reaction has energy barrier of 33.6 kcal/mol and consists of the following steps: (1) Nucleophilic substitution at acetyl chloride by the platinum of the reactant **A** forms five-coordinate Pt(IV) acylplatinum complex **B** with an energy barrier of 21.7 kcal/mol. (2) **B** undergoes 1,2-acyl migration from the platinum to the cyclometalated carbon through a three-membered platinacycle transition state to give Pt-arene η^2-complex **E** with an energy barrier of 14.0 kcal/mol. (3) **E** undergoes ligand exchange with chloride to form neutral Pt-arene η^2-complex **F**. (4) **F** undergoes ligand substitution with acetonitrile to give the product and the energy barrier is small (10.6 kcal/mol). The rate-determining step is the 1,2-acyl migration step. It is interesting to note that intermediate **F** was not included in the proposed mechanism but was identified by the NEB simulations. Five-coordinate Pt(IV) acylplatinum complex **B** undergoes barrierless ligand coordination with chloride to form neutral formal oxidative addition acylplatinum complex **D**; however, **D** is less stable than reactant **A** by 2.9 kcal/mol, which also implies that the isolation of an oxidative addition product Pt(IV) complex may be very challenging. The direct reductive elimination of **D** to form product **P** has a higher energy barrier (36.6 kcal/mol).

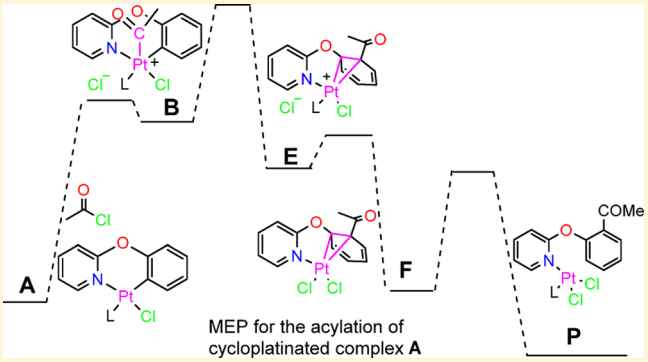

INTRODUCTION

Transition metal catalyzed C−H bond functionalization has attracted a great deal of attention, and platinum has played an important role in the chemistry of organometallic C−H activation and functionalization.[1] Owing to relatively stable C−Pt bond which allows for the isolation and characterization of key platinum intermediates, platinum systems are frequently used as models for mechanistic studies of the C−H activation.[2] In contrast, as a catalyst, platinum receives much less attention than its counterpart palladium because the stronger Pt−C bond would make its functionalization more difficult. However, this trend by no means suggests that platinum is inferior to other metals in all catalytic reactions. In fact, several recent publications indicate that the platinum catalyzed C−H functionalization has its own unique features,[3−8] demonstrating quite different reactivity and selectivity from other metals in catalytic hydroxylation of amines,[5] arene borylation,[6,7] and efficient hydroarylation of unsaturated hydrocarbons.[3,4,8]

In 2017, Huo's group reported a novel Pt-catalyzed acylation of 2-aryloxypyridines through direct C−H activation (Scheme 1).[9] Unlike other metal-catalyzed C−H acylation reactions, neither an oxidant nor other additives are required in this reaction, indicating that the Pt-catalyzed C−H acylation reaction may be mechanistically different from other reactions. On the basis of our previous investigation of Pt-mediated

Scheme 1. Pt-Catalyzed C−H Acylation of 2-Aryloxypyridines

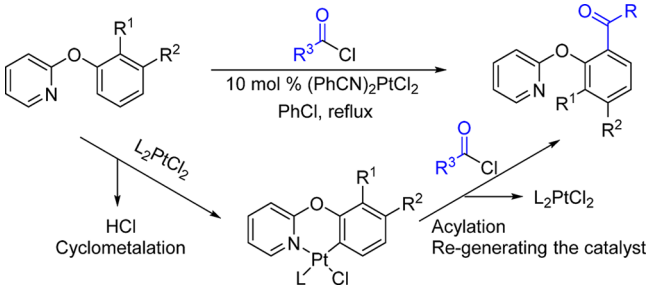

Received: September 23, 2019
Published: December 13, 2019

DOI: 10.1021/acs.inorgchem.9b02835
Inorg. Chem. 2020, 59, 555−562

Scheme 2. Possible Reaction Pathways for the Acylation of Cycloplatinated Complex A

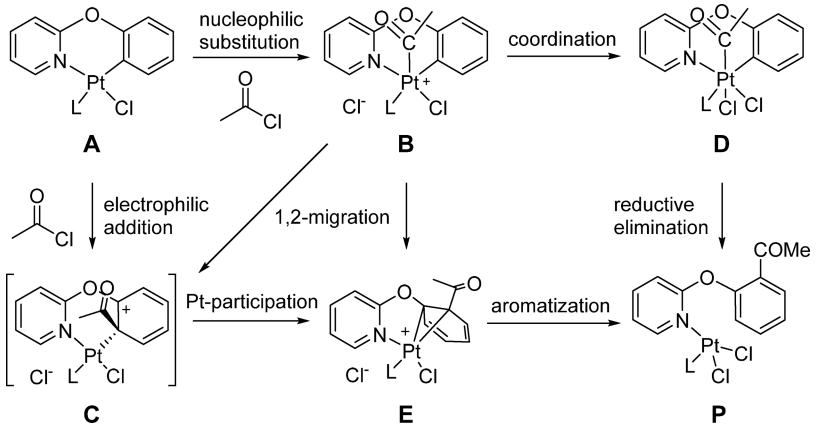

selective C−H activation and regiospecific acylation of cycloplatinated complexes,[10] it is quite clear that the Pt-catalyzed C−H acylation reaction proceeds in two distinct reactions: cyclometalation and acylation of cycloplatinated complex. Although the mechanism of Pt-catalyzed C−H activation reactions has been extensively studied both experimentally and theoretically,[2] very little is known about the mechanism of the acylation reaction. In this report, density functional theory (DFT) and nudged elastic band (NEB) theories will be used to study possible reaction pathways of the key acylation reaction of a cyclometalated platinum complex.[11]

COMPUTATIONAL METHODS

Geometry Optimization. All starting structures were built using Materials Studio and optimized with the program Gaussian 16 (G16)[12] on a computer cluster of 320 processors at East Carolina University. Two hybrid functionals were initially tried to see which method provided the best results both structurally and energetically for all platinum complexes. A new hybrid Meta exchange-correlation functional, M06-2X,[13] and a General Gradient Approximations (GGA) from Becke-3-Lee−Yang−Parr, B3LYP,[14] were compared. M06-2X in comparison to B3LYP showed similar structural features, but it had lower energy in gaseous phase simulations. Therefore, the mechanistic study of the complex structures prevailed with optimization using M06-2X. By the term complex, it is in reference to the optimized species with the leaving group present, which results in an overall neutral charge. For platinum, both *f* and *g* polarization functions are included in the def2-TZVP[15] basis set. All other atoms were optimized with the 6-311+g** basis set.[16] A polarizable continuum model (PCM)[17] is the default for the self-consistent reaction field (SCRF) method[18] and was employed for all calculations. Chlorobenzene was the medium used to simulate all calculations to be consistent with the experimental environment. Optimization was initially performed in a closed-shell environment. Open shell was tried as well, with the first 48 h of simulation, through mixing orbitals under a semiempirical INDO Hamiltonian,[19] followed with further optimization without those features until convergence was met. Final geometry optimization, energy calculations, and Mulliken analysis for reactants, intermediates, transition states, and products were carried out using G16 at a DFT level with the M06-2X functional and def2-TZVP basis set for Pt and 6-311+g** for all other atoms (M06-2X/def2-TZVP-Pt/6-311+g**). The solvent effects were simulated with the PCM using the integral equation formalism variant.

Frequencies. Force and vibrational frequencies for all optimized structures were calculated for all the structures. Force constants are determined based on the first derivative available, while vibrational frequencies are computed from the second derivative of the energies with respect to Cartesian nuclear coordinates.[20] The completed frequency calculation will include numerous types of data such as frequencies, intensities, associated normal modes, the structure's zero-point energy, and various thermo-chemical properties. The same level of theory preformed for optimization was used to run all frequency calculations. All the stable structures were confirmed with all the positive frequencies and the transition state structures were confirmed with only one imaginary frequency.

Potential Energy Profile Simulation Using NEB. The NEB[21] method maps the reaction pathway between two optimized stationary points on a potential energy surface. Each NEB calculation was run with a fire optimizer[21c] and a string of either 22 or 13 images, based upon the complexity of the reaction step, until the desired structures (transition states and intermediates) were refined. To grasp a more identifiable transition state peak from the simulation, the climbing image[22] feature in NEB calculations was turned on around cycle 300 and ran until cycle 450 to avoid over- or under-shooting the true transition state(s). The reaction pathway between the optimized complexes invoked the orbital mixing for the first 12 cycles. NEB calculations were all performed using M06-2X/def2-TZVP-Pt/6-311+g** level of theory in G16. All NEB calculations employed the polarizable continuum model, with chlorobenzene as the solvent.

Transition State Optimization. Following NEB simulations, we employed a few different min-mode following methods. The dimer method,[23a,b] developed by Henkelman, is a method for finding transition states using only gradients. Two points were chosen from the reaction pathway as the starting points for the dimer optimization method. The chosen points were images closest to the highest peak from the NEB curve. Both the transition state point, R_0, and another point closet, R_1, were chosen as a pair or two points surrounding the highest point, R_1 and R_2, were selected. Dimer optimization was run with M06-2X/def2-TZVP-Pt/6-311+g** level of theory. Additional Gaussian transition state optimization was employed as well for comparison. Two techniques were used: (1) the Synchronous Transit-Guided Quasi-Newton (STQN) Method,[24] developed by Schlegel and co-workers, known as QST2, and (2) TS optimization request which uses the Berny algorithm.[25] The first technique was generated similar to the dimer method, inputting two points either including the transition state or the two nearest points. The second technique was run in conjunction with the dimer method, using the optimized saddle point coordinates for simulation. Following optimization, all transitions states were verified based on their frequency calculations at the same level of theory.

RESULT AND DISCUSSION

Proposed Mechanism. In 1981 and 1983, Holton[26] and Clark[27] reported a stoichiometric acylation of cyclometalated palladium complexes by using acyl chlorides, but a catalytic version of the acylation reaction has never been reported. Both oxidative addition/reductive elimination[26] and insertion/elimination[27] mechanisms were proposed for the stoichio-

DOI: 10.1021/acs.inorgchem.9b02835
Inorg. Chem. 2020, 59, 555−562

metric acylation of cyclopalladated complexes. Although our previous study on the stoichiometric acylation reaction of tridentate C^N^N-coordinated platinum complexes[11] does not seem to support a simple oxidative addition/reductive elimination or the insertion/elimination mechanism proposed for the acylation of cyclometalated palladium complexes, we cannot rule out this mechanism in the catalytic reaction. In the Pt-catalyzed C−H acylation reaction, the substituent electronic effect demonstrated that more electron-deficient acyl chlorides substantially enhanced the reaction,[9] which strongly suggests a nucleophilic attack at the acyl chloride by the cycloplatinated complex. Therefore, we proposed the following possible reaction pathways (Scheme 2) for our computational study.

We use the acylation of cycloplainated complex **A** (L = a ligand) with acetyl chloride as our model reaction for the computational study. In the actual Pt-catalyzed C−H acylation, ligand L could be either benzonitrile, which is from the catalyst $Pt(PhCN)_2Cl_2$, or a 2-aryloxypyridine compound (either the reactant or the acylated product). To simplify the model, we use acetonitrile to replace ligand L. It is reasonable to assume that the acylation reaction is triggered by nucleophilic attack at acetyl chloride in two different ways: (1) by the platinum (**A** to **B**) via a classical nucleophilic substitution at acyl chlorides which is also considered to be an oxidative addition in terms of the change of oxidative state of the platinum and (2) by the electron-rich metalated benzene (**A** to **C**), which is analogy to electrophilic aromatic substitution. Five-coordinated intermediate **B** can be either trapped by the chloride to form formal oxidative addition product **D** or undergo 1,2-acyl migration from the Pt to the metalated carbon to form arenium ion **C**. Alternatively, electrophilic addition of metalated benzene to the acyl chloride could lead to the formation of **C**. Arenium ion **C** undergoes the rearomatization to give acylated product **P**. However, all of efforts to optimize proposed arenium ion intermediate **C** lead to structure **E** (see the discussion in the following section), which can be treated either as a Pt-arene η^2-complex or a platinacyclopropane. Therefore, our proposed possible pathways for the computational study include intermediate **E**, which can be formed by either 1,2-mirgation of acyl group of **B** or formal electrophilic addition of metalated benzene. Intermediate **E** undergoes rearomatization or ligand substitution to form product **P**. Reductive elimination of **D** would directly lead to product **P**.

Optimization of Proposed Structures. Our initial efforts were devoted to optimizing the proposed stable structures including reactant **A**, product **P**, and proposed intermediates **B**−**D**. This has proven to be very informative and fruitful. For example, the optimization of proposed arenium ion intermediate **C** automatically collapsed to produce structure **E** (Scheme 3). Although the arenium ion formed for an analogous aromatic electrophilic substitution of electron-rich pincer cycloplatinated complex is known and the structure has been determined by X-ray crystallography,[28] theoretically, arenium ion **C** does not exist! Apparently, arenium ion **C**, if formed, would be stabilized through the platinum participation to form structure **E** (Scheme 3). All other proposed structures are confirmed to be minima by the frequency calculations, and all of them have positive vibrational frequencies. The optimized structures of **A**, **B**, **D**, **E**, and **P** are shown in Figure 1, and their selected bond distances and bond angles are listed in Table 1.

Scheme 3. Stabilization of Arenium Ion through Pt Participation

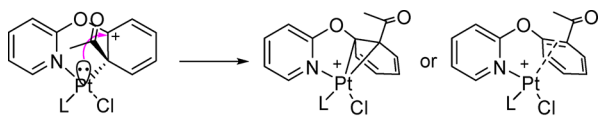

Structure **E** can be described either as a platinacyclopropane or as a cationic platinum-arene η^2-complex. It should be mentioned that cationic platinum-arene η^2-complexes have been considered as the important intermediate in the Pt-mediated arene C−H activation reaction,[29] and the X-ray crystal structure of such a platinum-arene η^2-complex has been reported. The lengths of the two Pt−C1 and Pt−C3 bonds in **E** are 2.299 and 2.343 Å, respectively, which are similar to those found in the crystal structure of a previously reported Pt-arene η^2-complex (2.317 and 2.390 Å).[29] The C1−Pt−C3 angle is 35.8°, which is also similar to that reported previously (34.3°).[29] The angle between the platinacyclopropane and the benzene ring is 75.0°, which is significantly smaller than that found in a normal Pt-arene π−η^2-complex which is much closer to 90°.[29] The phenyl ring remains planar. However, the alternation of bond lengths within the benzene ring indicates a considerable dearomatization effect caused by the Pt-coordination (Figure 2).

In the structure of **A**, the six-membered platinacycle displays a boat conformation, with the platinum and the oxygen linker being the flagpoles. The bidentate cyclometalated ligand has a bowing shape, bending away from the platinum and the oxygen linker. The platinum displays a nearly perfect square planar coordination geometry. The Pt−C1, Pt−N1, and Pt−Cl1 are all in the normal range. The Pt−N2 bond is slightly longer than the Pt−N1 bond because of the trans effect of the carbon donor. Five-coordinate **B** is a highly reactive intermediate, 19.62 kcal/mol above reactant **A**. Five-coordinate Pt(IV) species have been reported by Rourke and co-workers.[30] The cationic five-coordinate complex displays a nearly perfect square pyramidal geometry. Six-coordinate platinum(IV) complex **D** has an octahedral coordination geometry. The Pt−Cl2 bond (2.586 Å) is significantly longer than the Pt−Cl1 bond (2.3334 Å). In addition to the trans effect exerted by the carbonyl ligand, the steric hindrance might also play a role because the bowing shape of the bidentate cyclometalated ligand may restrict the chloride Cl2 from approaching the platinum. Oxidative addition product **D** is less stable than the reactant by 2.9 kcal/mol. Pt-arene complex **E** is more stable than five-coordinate intermediate **B** by 4.6 kcal/mol. Product *trans*-**P** is the more stable trans isomer with square planar geometry, which is 12.1 kcal/mol more stable than reactant **A**. The cis isomer was also optimized, but it is 3.1 kcal/mol higher than the trans isomer. Overall, the acylation reaction is thermodynamically favorable.

Mapping Reaction Pathways Using NEB. With the optimized minima, NEB calculations were used to find the minimum energy pathway (MEP) and the saddle point between two minima. The results will be analyzed to elucidate the mechanism of the acylation reaction. Our first round of NEB simulations were performed to find the MEPs for the following conceived elementary reaction steps: **A** → **B** (nucleophilic substitution/oxidative addition), **A** → **D** (concerted oxidative addition), **B** → **E** (1,2-acyl migration),

DOI: 10.1021/acs.inorgchem.9b02835
Inorg. Chem. 2020, 59, 555−562

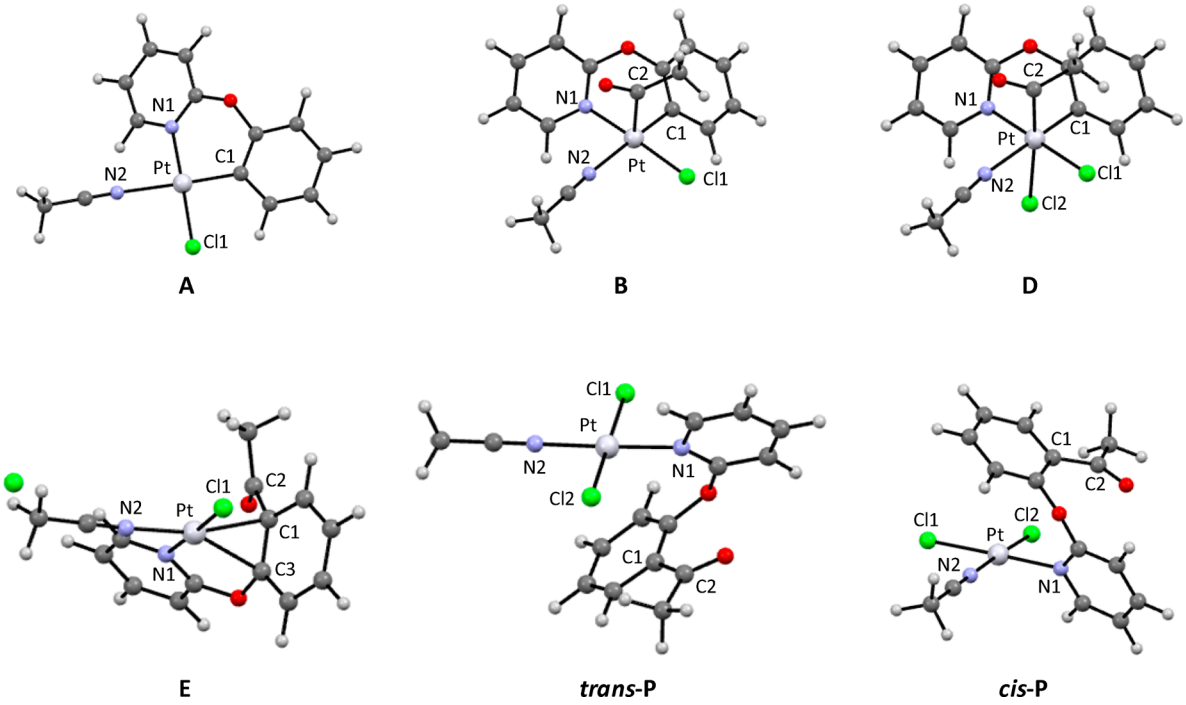

Figure 1. Optimized structures of **A**, **B**, **D**, **E**, and *trans*- and *cis*-**P**.

Table 1. Bond Lengths (Å) and Angles (degree) of Optimized Structures

structure	A	B	D	E	*trans*-P	*cis*-P
Pt−C1	1.959	1.979	1.975	2.299		
Pt−C2		2.055	2.026			
Pt−C3				2.343		
Pt−N1	2.056	2.063	2.065	2.044	2.045	2.077
Pt−N2	2.202	2.239	2.248	2.016	1.997	2.012
Pt−Cl1	2.361	2.330	2.334	2.333	2.351	2.325
Pt−Cl2			2.586		2.351	2.313
C1−Pt−N2	177.1	175.8	178.5			
Cl1−Pt−N1	177.1	177.6	178.5	178.0	89.0	178.8
C1−Pt−N1	88.2	87.3	87.3	86.4		
C1−Pt−C2		93.9	91.5			
C1−Pt−Cl2			92.6			
C1−Pt−C3				35.8		
Cl1−Pt−Cl2			92.6		177.0	91.9
N1−Pt−N2	91.2	91.7	92.0	91.5	178.3	89.9

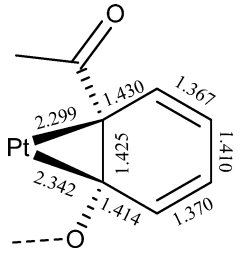

Figure 2. Key structure parameters of intermediate **E** showing the alternation of C−C bond lengths (Å).

B → **D** (ligand substitution/trapping of five-coordinate Pt(IV) species **B**), **E** → **P** (ligand substitution/rearomatization), and **D** → **P** (reductive elimination). The optimized geometries for transition states $\mathbf{TS_{AB}}$, $\mathbf{TS_{BE}}$, $\mathbf{TS_{DP}}$, and $\mathbf{TS_{AD}}$ are shown in Figure 3, which also shows the structural parameters for the partial structure of $\mathbf{TS_{BE}}$.

Formation of Five-Coordinated Intermediate B. The formation of **B** can be either considered as the first step of oxidative addition or a classical nucleophilic substitution of the acyl chloride. The NEB simulation produced a unique MEP with an initial sharp increase of potential energy (Figure 4), which was identified as the dissociation of the C−Cl bond of the acetyl chloride. The geometry of transition state $\mathbf{TS_{AB}}$ ($\mathbf{TS_{AB}}$, Figure 3) also indicates that the dissociation of the C−Cl bond (2.547 Å in $\mathbf{TS_{AB}}$ vs 1.822 Å in acetyl chloride) is almost complete whereas the C_{acyl}−Pt bond has not been fully formed (2.373 Å in $\mathbf{TS_{AB}}$ vs 2.054 Å in **B**). The beginning of the reaction is essentially to form the acylium ion. The activation energy is 21.7 kcal/mol.

We also consider a conventional nucleophilic addition of the Pt to the acetyl chloride to form a tetrahedral intermediate, which is very common in the nucleophilic addition/elimination mechanism proposed for nucleophilic substitution of acyl chlorides in organic chemistry. However, the optimization of

DOI: 10.1021/acs.inorgchem.9b02835
Inorg. Chem. 2020, 59, 555−562

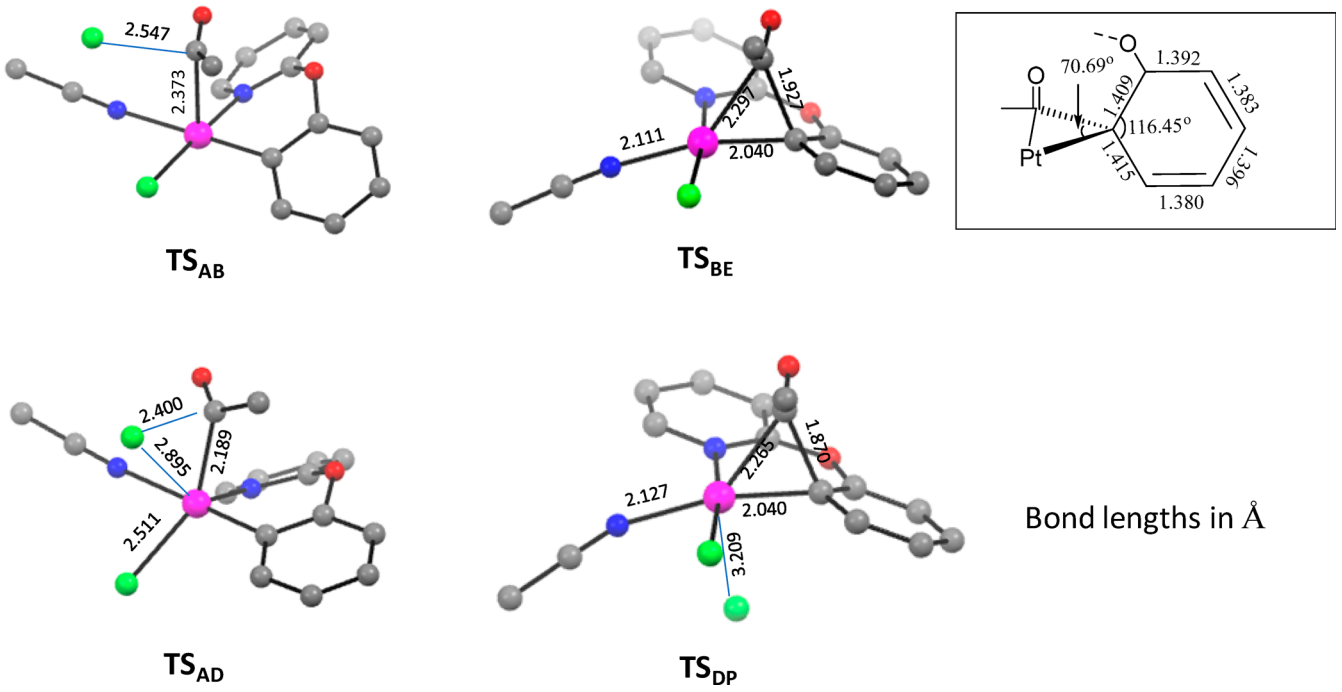

Figure 3. Optimized structure of the transition state TS_{AB}, TS_{BE}, TS_{AD}, and TS_{DP}. Shown in the box are the structural parameters for the partial structure of TS_{BE}.

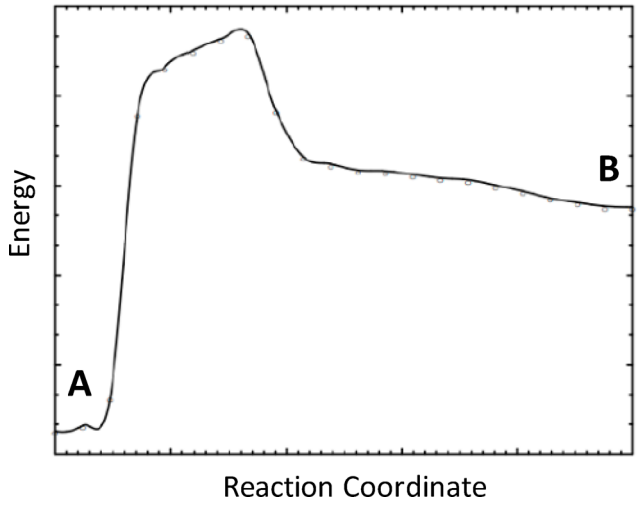

Figure 4. NEB simulated MEP for the conversion of **A** to **B**.

such tetrahedral intermediate was not successful, presumably due to the steric hindrance induced by the square planar Pt complex. It should be mentioned that the simulation of a pathway involving the nucleophilic attack by the metalated carbon to form a C−C bond was also attempted, but the acyl group always slips to form the C−Pt bond (intermediate **B**).

Formation of Oxidative Addition Product D. Trapping of five-coordinated intermediate **B** by a chloride is essentially a downhill process with only very small activation energy (1.7 kcal/mol) to form oxidative addition product **D**, which is predicted to be a stable octahedral Pt(IV) complex. As a comparison, the NEB simulation was also performed for a concerted oxidative addition pathway **A** → **D**, but the energy barrier (36.6 kcal/mol) is much higher than that of two step pathway **A** → **B** → **D** (21.7 kcal/mol). The concerted pathway involves a three-center transition state, TS_{AD}, as shown in Figure 3.

The NEB simulation suggests that reactant **A** and oxidative addition product **D** are in equilibrium through highly reactive intermediate **B**, but favorable to the reactant. The barriers for the conversion of **B** to **A** and **B** to **D** are both very small, 2.1 and 1.7 kcal/mol, respectively; therefore, **B** must be a short-lived intermediate.

1,2-Migration of Acyl Group from Pt to Carbon. Formation of the C−C bond must involve the migration of the acyl group from the Pt to the metalated carbon. Our previous study of regiospecific acylation of cycloplatinated complexes already confirmed that the acylation occurs at the metalated carbon.[10b] Therefore, it must be a 1,2-migration process, which has been suggested in other Pt-mediated C−H activation and functionalization reactions.[2] The NEB simulation on the reaction **B** → **E** located transition state TS_{BE} for the migration reaction which is a three-center species with the carbonyl carbon bridging the platinum and the metalated carbon (TS_{BE}, Figure 3). The three-membered platinacycle is perpendicular to the phenyl ring (85.7°). The metalated carbon displays a distorted tetrahedral geometry with C2−C1−Pt bond angle of 70.7°. Dearomatization has occurred at the transition state indicated by the change of bond distance in the phenyl ring (Figure 3). Other notable feature is the change in the Pt−N2 bond trans to metalated carbon in **B**, which is shorter in the transition state because of the diminishing of the trans effect as the C−Pt bond becomes longer and is no longer linear with the Pt−N2 bond (166.8°). Although arenium ion **C** does not exist as a stable intermediate, transition state TS_{BE} resembles **C** in many ways, especially its distorted tetrahedral geometry and the dearomatization of the benzene ring. The Pt−C3 distance (2.953 Å) in TS_{BE} is essentially the same as that of **B** (2.911 Å), indicating that arenium species (**C**-like) might be formed first, then trapped by the Pt to form the platinacyclopropane or

DOI: 10.1021/acs.inorgchem.9b02835
Inorg. Chem. 2020, 59, 555−562

Pt-arene complex **E**. The energy barrier for the 1,2-migration is 14.0 kcal/mol.

Reductive Elimination of D. The simple oxidative addition and reductive elimination mechanism has been frequently proposed for the transition metal-catalyzed C−H functionalization reactions. Reductive elimination from oxidative addition product **D** was evaluated by the NEB simulation. Surprisingly, the energy barrier for this concerted reduction elimination is very high at 33.7 kcal/mol. Transition state $\mathbf{TS_{DP}}$ features in a three-membered platinacycle and a significantly elongated Pt−Cl bond (3.209 Å) (Figure 3). Except for the dissociated chloride, the geometry of transition state $\mathbf{TS_{DP}}$ is nearly identical to that of $\mathbf{TS_{BE}}$ which leads to the formation of Pt-arene η^2-π-complex **E**. However, $\mathbf{TS_{DP}}$ is less stable than $\mathbf{TS_{BE}}$ by 3 kcal/mol. The energy difference may be attributed to the elongated Pt−Cl bond in $\mathbf{TS_{DP}}$, while in $\mathbf{TS_{BE}}$ the chloride is a spectator ion (fully dissociated) that does not induce any strain. The significant elongation of the Pt−Cl bond in $\mathbf{TS_{DP}}$ also suggests that the dissociation of the Pt−Cl is the driving force for the reductive elimination.

Rearomatization of E to Form the Product P. The formation of the product from intermediate **E** can be considered as a rearomatization process through reductive elimination of platinacyclopropane or a ligand substitution of the Pt-arene complex with a chloride, which should not involve any significant kinetic barrier. However, the NEB simulation of the reaction pathways for converting **E** to *trans*-**P** has been troublesome. Preliminary NEB simulation indicated a relatively low barrier, but the optimization of the transition state has not been successful. Then we thought that converting **E** to *cis*-**P** might be more reasonable because in the initial structure of reactant **A** the acetonitrile ligand is cis to the pyridinyl nitrogen. Therefore, a NEB simulation was performed on converting **E** to *cis*-**P**. Quite surprisingly, the simulation produced a potential energy curve indicating a new intermediate, **F** (Figure 5).

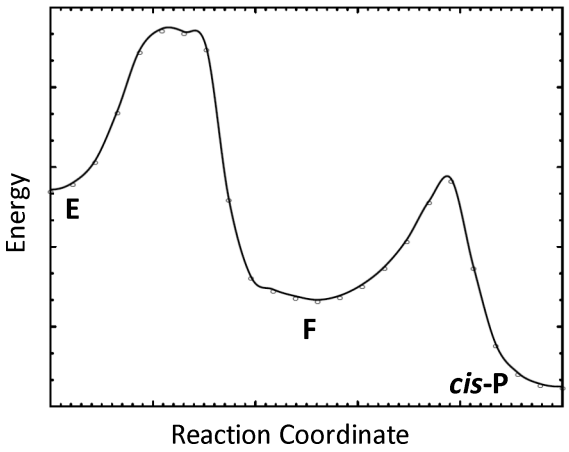

Figure 5. NEB simulated MEP for converting **E** to *cis*-**P**.

The optimized structure of **F** displays an interesting structure of intramolecular η^2-Pt-arene complex (Figure 6), or it can be treated as a platinacyclopropane with two Pt−C bonds being nearly identical (2.299 and 2.295 Å for Pt−C1 and Pt−C3, respectively). The C1−C3 bond is 1.427 Å, which is significantly longer than the C−C bond in benzene. The benzene ring has an alteration of the C−C bond lengths (Figure 6) similar to conjugated diene structure, which indicates significant dearomatization of the benzene ring. This structure is also similar to cationic platinum-arene η^2-complex **E**. The dihedral angle between the platinacycle and the benzene ring is 106.1°. There have been reports of platinum complexes displaying an intramolecular arene−platinum interaction, and their X-ray crystal structures have been determined,[31] which are similar to the optimized structure of **F**. The identification of intermediate **F** also demonstrated the power of the NEB method.

Transition state $\mathbf{TS_{FP}}$ for the conversion from **F** to *cis*-**P** was located and the structure is shown in Figure 6. The energy barrier (not zero-point energy corrected) is 10.6 kcal/mol. The normal mode along the TS path was very soft (30/1 cm; within the numerical noise). Since this mode is so soft, the zero-point energy corrected barrier is 10.6 kcal/mol (nearly the same as uncorrected zero-point energy corrected energy). This is a fast reaction ($k = 1.014 \times 10^5$ s^{-1}). This mode was a mainly a movement of the chlorine along an arc (Cl−Pt) with the bond distance changing little. That is, the C−N−Pt-Cl dihedral angle changes. The acetonitrile ligand remains dissociated (Pt−N distance of 3.054 Å). The TS is a rotation. As the Cl gets to a C−N−Pt−Cl angle around 67°, the acetonitrile ligand may undergo a barrierless coordinating to the Pt. However, the transition state for the conversion of **E** to **F** is difficult to locate. Using the dimer optimization method always leads to either **E** or **F**.

Lowest Energy Pathway for the Acylation Reaction. Figure 7 illustrates the comparison of different MEPs for the acylation reaction. It is obvious that the simple oxidative-addition−reductive-elimination mechanism **A** → **D** → **P** (Figure 7, in red) is unlikely, because both the concerted oxidative and the reductive elimination each have very large barrier (36.6 kcal/mol) to overcome. Especially, the conversion of oxidative addition product **D** to more stable reactant **A** via intermediate **B** has a much smaller barrier (18.8 kcal/mol) than that for the conversion to the product **P** though the direct reductive elimination. The lowest energy pathway for the formation of oxidative addition product **D** is stepwise via five-coordinate platinum species **B**, which should be more accurately characterized as the nucleophilic substitution of acyl chloride and ligand association, **A** → **B** → **D**. The lowest energy pathway is identified as **A** → **B** → **E** → **F** → **P**, with an energy barrier of 33.6 kcal/mol. The rate-determining step is the 1,2-migration of the acyl group from the platinum to the metalated carbon.

CONCLUSION

The acylation of the cycloplatinated complex is a key step of the catalytic cycle in the unique Pt-catalyzed direct C−H acylation with acyl chlorides. A DFT study has been performed for the first time to elucidate the mechanism of the acylation reaction. The NEB simulation of possible reaction pathways suggests that the acylation reaction proceeds with four elementary steps: (1) nucleophilic substitution of the acyl chloride to form five-coordinate acylplatinum complex, (2) 1,2-migration of the acyl group from the platinum to the metalated carbon to form a cationic Pt-arene η^2-complex or platinacyclpropane, (3) ligand exchange with chloride to form a neutral Pt-arene η^2-complex or platinacyclpropane, and (4) dissociation of the Pt-arene complex or rearomatization of the platinacyclopropoane through ligand substitution by acetonitrile ligand. The five-coordinate species is the key intermediate because the direct oxidative addition/reductive elimination

DOI: 10.1021/acs.inorgchem.9b02835
Inorg. Chem. 2020, 59, 555−562

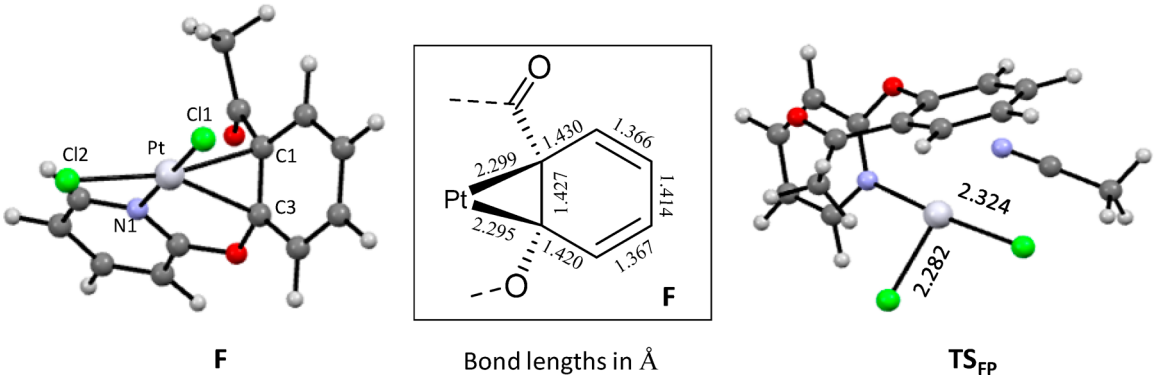

Figure 6. Optimized structures of intermediate **F** and transition state $\mathbf{TS_{FP}}$.

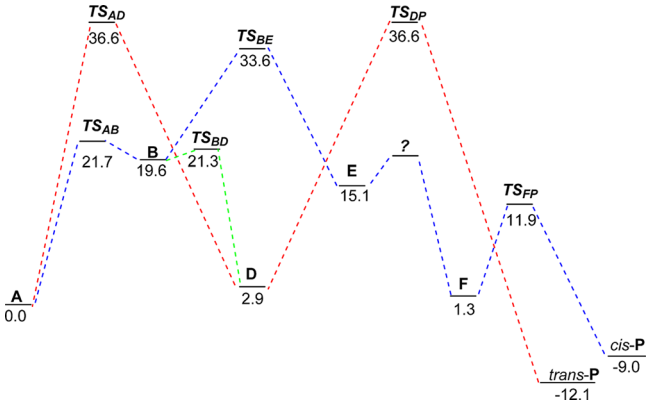

Figure 7. Schematic energy (kcal/mol) diagrams of possible mechanisms of the acylation reaction. Lowest energy pathway is highlighted in blue.

involve a higher energy barrier. The 1,2-acyl migration is the rate-determining step. This study should also help understand other metal-catalyzed aromatic C−H acylation reactions when an acyl metal species is involved in the mechanism.

■ ASSOCIATED CONTENT

Supporting Information

The Supporting Information is available free of charge at https://pubs.acs.org/doi/10.1021/acs.inorgchem.9b02835.

Computed molecule Cartesian coordinates (PDF)

■ AUTHOR INFORMATION

Corresponding Authors

*E-mail: liyu@ecu.edu (Y.L.).

*E-mail: huos@ecu.edu (S.H.).

ORCID

Shouquan Huo: 0000-0001-9516-4013

Yumin Li: 0000-0003-2183-5317

Notes

The authors declare no competing financial interest.

■ ACKNOWLEDGMENTS

We thank the National Science Foundation (NSF-CHE-1900102) for financial support of this research.

■ REFERENCES

(1) Labinger, J. A. Platinum-Catalyzed C−H Functionalization. *Chem. Rev.* **2017**, *117*, 8483−8496.

(2) Lersch, M.; Tilset, M. Mechanistic Aspects of C−H Activation by Pt Complexes. *Chem. Rev.* **2005**, *105*, 2471−2526.

(3) McKeown, B. A.; Gonzalez, H. E.; Friedfeld, M. R.; Gunnoe, T. B.; Cundari, T. R.; Sabat, M. Mechanistic Studies of Ethylene Hydrophenylation Catalyzed by Bipyridyl Pt(II) Complexes. *J. Am. Chem. Soc.* **2011**, *133*, 19131−19152.

(4) McKeown, B. A.; Gonzalez, H. E.; Michaelos, T.; Gunnoe, T. B.; Cundari, T. R.; Crabtree, R. H.; Sabat, M. Control of Olefin Hydroarylation Catalysis via a Sterically and Electronically Flexible Platinum(II) Catalyst Scaffold. *Organometallics* **2013**, *32*, 3903−3913.

(5) Lee, M.; Sanford, M. S. Platinum-Catalyzed, Terminal-Selective C(sp^3)−H Oxidation of Aliphatic Amines. *J. Am. Chem. Soc.* **2015**, *137*, 12796−12799.

(6) Furukawa, T.; Tobisu, M.; Chatani, N. C−H Functionalization at Sterically Congested Positions by the Platinum-Catalyzed Borylation of Arenes. *J. Am. Chem. Soc.* **2015**, *137*, 12211−12214.

(7) Takaya, J.; Ito, S.; Nomoto, H.; Saito, N.; Kirai, N.; Iwasawa, N. Fluorine-controlled C−H Borylation of Arenes Catalyzed by a PSiN-pincer Platinum Complex. *Chem. Commun.* **2015**, *51*, 17662−17665.

(8) Clement, M. L.; Grice, K. A.; Luedtke, A. T.; Kaminsky, W.; Goldberg, K. I. Platinum(II) Olefin Hydroarylation Catalysts: Tuning Selectivity for the anti-Markovnikov Product. *Chem. - Eur. J.* **2014**, *20*, 17287−17291.

(9) McAteer, D. C.; Javed, E.; Huo, L.; Huo, S. Platinum-Catalyzed Double Acylation of 2-(Aryloxy)pyridines via Direct C−H Activation. *Org. Lett.* **2017**, *19*, 1606−1609.

(10) (a) Carroll, J.; Gagnier, J. P.; Garner, A. W.; Moots, J. G.; Pike, R. D.; Li, Y.; Huo, S. Reaction of N-Isopropyl-N-phenyl-2,2'-bipyridin-6-amine with K_2PtCl_4: Selective C−H Bond Activation, C−N Bond Cleavage, and Selective Acylation. *Organometallics* **2013**, *32*, 4828−4836. (b) Carroll, J.; Woolard, H. G.; Mroz, R.; Nason, C. A.; Huo, S. Regiospecific Acylation of Cycloplatinated Complexes. Scope, Limitations, and Mechanistic Implications. *Organometallics* **2016**, *35*, 1313−1322.

(11) McPherson, K. E.; Bartolotti, L. J.; Morehead, A. T.; Sargent, A. L. Utility of the Nudged Elastic Band Method in Identifying the Minimum Energy Path of an Elementary Organometallic Reaction step. *Organometallics* **2016**, *35*, 1861−1865.

(12) Frisch, M. J.; Trucks, G. W.; Schlegel, H. B.; Scuseria, G. E.; Robb, M. A.; Cheeseman, J. R.; Scalmani, G.; Barone, V.; Petersson, G. A.; Nakatsuji, H.; Li, X.; Caricato, M.; Marenich, A. V.; Bloino, J.; Janesko, B. G.; Gomperts, R.; Mennucci, B.; Hratchian, H. P.; Ortiz, J. V.; Izmaylov, A. F.; Sonnenberg, J. L.; Williams-Young, D.; Ding, F.; Lipparini, F.; Egidi, F.; Goings, J.; Peng, B.; Petrone, A.; Henderson, T.; Ranasinghe, D.; Zakrzewski, V. G.; Gao, J.; Rega, N.; Zheng, G.; Liang, W.; Hada, M.; Ehara, M.; Toyota, K.; Fukuda, R.; Hasegawa, J.; Ishida, M.; Nakajima, T.; Honda, Y.; Kitao, O.; Nakai, H.; Vreven, T.; Throssell, K.; Montgomery, J. A., Jr.; Peralta, J. E.; Ogliaro, F.; Bearpark, M.; Heyd, J. J.; Brothers, E. N.; Kudin, K. N.; Staroverov, V. N.; Kobayashi, R.; Normand, J.; Raghavachari, K.; Rendell, A.; Burant, J. C.; Iyengar, S. S.; Tomasi, J.; Cossi, M.; Millam, J. M.; Klene, M.; Adamo, C.; Cammi, R.; Ochterski, J. W.; Martin, R. L.; Morokuma,

DOI: 10.1021/acs.inorgchem.9b02835
Inorg. Chem. 2020, 59, 555−562

K.; Farkas, O.; Foresman, J. B.; Fox, D. J. *Gaussian 16*, revision B.01; Gaussian, Inc.: Wallingford CT, 2016.
(13) Zhao, Y.; Truhlar, D. G. The M06 Suite of Density Functionals for Main Group Thermochemistry, Kinetics, Noncovalent Interactions, Excited states, and Transition Elements: Two New Functionals and Systematic Testing of Four M06 Functionals and Twelve Other Functionals. *Theor. Chem. Acc.* **2008**, *120*, 215−241.
(14) Becke, A. D. Density-Functional Thermochemistry. III. The Role of Exact Exchange. *J. Chem. Phys.* **1993**, *98*, 5648−52.
(15) Weigend, F.; Ahlrichs, R. Balanced Basis Sets of Split Valence, Triple Zeta Valence and Quadruple Zeta Valence Quality for H to Rn: Design and Assessment of Accuracy. *Phys. Chem. Chem. Phys.* **2005**, *7*, 3297−3305.
(16) (a) Binning, R. C., Jr.; Curtiss, L. A. Compact Contracted Basis-sets for 3rd-Row Atoms − GA-KR. *J. Comput. Chem.* **1990**, *11*, 1206−16. (b) McGrath, M. P.; Radom, L. Extension of Gaussian-1 (G1) Theory to Bromine-containing Molecules. *J. Chem. Phys.* **1991**, *94*, 511−16. (c) Curtiss, L. A.; McGrath, M. P.; Blaudeau, J.-P.; Davis, N. E.; Binning, R. C., Jr.; Radom, L. Extension of Gaussian-2 Theory to Molecules Containing Third-row Atoms Ga-Kr. *J. Chem. Phys.* **1995**, *103*, 6104−13.
(17) (a) Improta, R.; Barone, V.; Scalmani, G.; Frisch, M. J. A State-specific Polarizable Continuum Model Time Dependent Density Functional Method for Excited State Calculations in Solution. *J. Chem. Phys.* **2006**, *125*, No. 054103. (b) Improta, R.; Scalmani, G.; Frisch, M. J.; Barone, V. Toward effective and reliable fluorescence energies in solution by a new State Specific Polarizable Continuum Model Time Dependent Density Functional Theory Approach. *J. Chem. Phys.* **2007**, *127*, 074504.
(18) Tomasi, J.; Mennucci, B.; Cammi, R. Quantum Mechanical Continuum Solvation Models. *Chem. Rev.* **2005**, *105*, 2999−3093.
(19) Pople, J. A.; Beveridge, D.; Dobosh, P. Approximate Self-consistent Molecular-orbital Theory. 5. Intermediate Neglect of Differential Overlap. *J. Chem. Phys.* **1967**, *47*, 2026−2033.
(20) Ochterski, J. W. *Vibrational Analysis in Gaussian*; Gaussian, Inc., 1999.
(21) (a) Sheppard, D.; Terrell, R.; Henkelman, G. Optimization Methods for Finding Minimum Energy Paths. *J. Chem. Phys.* **2008**, *128*, 134106. (b) Jónsson, H.; Mills, G.; Jacobsen, K. Nudged Elastic Band Method for Finding Minimum Energy Paths of Transition. *Proc. Int. Sch. Phys.* **1997**, 385−404. (c) Bitzek, E.; Koskinen, P.; Gahler, F.; Moseler, M.; Gumbsch, P. Simple Relaxation Made Simple. *Phys. Rev. Lett.* **2006**, *97*, 170201−4.
(22) Henkelman, G.; Uberuaga, B. P.; Jonsson, H. A Climbing Image Nudged Elastic Band Method for Finding Saddle Points and Minimum Energy Paths. *J. Chem. Phys.* **2000**, *113*, 9901−9904.
(23) (a) Henkelman, G.; Jónsson, J. A Dimer Method for Finding Saddle Points on High Dimensional Potential Surfaces using only First Derivatives. *J. Chem. Phys.* **1999**, *111*, 7010−7022. (b) Heyden, A.; Bell, A. T.; Keil, F. J. Efficient Methods for Finding Transition States in Chemical Reactions: Comparison of Improved Dimer Method and Partitioned Rational Function Optimization Method. *J. Chem. Phys.* **2005**, *123*, 224101−14.
(24) Peng, C.; Bernhard Schlegel, H. Combining Synchronous Transit and Quasi-Newton Methods for Finding Transition States. *Isr. J. Chem.* **1993**, *33*, 449−454.
(25) Li, X.; Frisch, M. J. Energy-represented DIIS within a Hybrid Geometry Optimization Method. *J. Chem. Theory Comput.* **2006**, *2*, 835−39.
(26) Holton, R. A.; Natalie, K. J., Jr. A New Regiospecific Synthesis of Aryl Ketones from Palladacycles. *Tetrahedron Lett.* **1981**, *22*, 267−270.
(27) Clark, P. W.; Dyke, H. J.; Dyke, S. F.; Perry, G. Palladium Assisted Organic Reactions. V. The Reactions of di-μ-Chloro-bis(N,N-diakylbenzylamine-2-C,N)dipalladium(II) Complexes with Acyl Chlorides. *J. Organomet. Chem.* **1983**, *253*, 399−413.
(28) Albrecht, M.; Spek, A. L.; van Koten, G. $C_{arenium}$−C_{alkyl} Bond Making and Breaking: Key Process in the Platinum-mediated C_{aryl}−C_{alkyl} Bond Formation. Analogies to Organic Electrophilic Aromatic Substitution. *J. Am. Chem. Soc.* **2001**, *123*, 7233−7246.
(29) Reinartz, S.; White, P. S.; Brookhart, M.; Templeton, J. L. Structural Characterization of An Intermediate in Arene C−H bond Activation and Measurement of the Barrier to C−H Oxidative Addition: A Platinum(II) η^2-Benzene Adduct. *J. Am. Chem. Soc.* **2001**, *123*, 12724−12725.
(30) (a) Shaw, P. A.; Clarkson, G. J.; Rourke, J. P. Long-Lived Five-Coordinate Platinum(IV) Intermediates: Regiospecific C−C Coupling. *Organometallics* **2016**, *35*, 3751−3762. (b) Shaw, P. A.; Phillips, J. M.; Clarkson, G. J.; Rourke, J. P. Trapping Five-coordinate platinum(IV) Intermediates. *Dalton Trans.* **2016**, *45*, 11397−11406.
(31) (a) Casas, J. M.; Fornies, J.; Martin, A.; Menjon, B. Synthesis, Solid-state and Solution Structure, and Reactivity of cis-[Pt-(C_6F_5)$_2$(NC_5H_4-2-$CH_2C_6H_5$)]: A Compound Displaying an Arene-Platinum Interaction. *Organometallics* **1993**, *12*, 4376−4380. (b) Casas, J. M.; Fornies, J.; Martin, A.; Menjon, B.; Tomas, M. Pentafluorophenylplatinum Complexes Containing η^1- or η^2-Aryl-Pt Interactions. Crystal Structure of *cis*-[Pt(C_6F_5)2-({NC_5H_4[CH(η^2-Ph)Ph]-2}-κN)]·0.5C_6H_6Me. *J. Chem. Soc., Dalton Trans.* **1995**, 2949−2954.

DOI: 10.1021/acs.inorgchem.9b02835
Inorg. Chem. 2020, 59, 555−562